# Effect of polymer architecture and acidic group density on the degree of salt formation in amorphous solid dispersions

Amy Lan Neusaenger, <sup>1</sup> Caroline Fatina, <sup>1</sup> Junguang Yu<sup>1</sup>, and Lian Yu<sup>1,2</sup>

- 1. University of Wisconsin, School of Pharmacy, Madison, WI 53705
- 2. University of Wisconsin, Department of Chemistry, Madison, WI 53706

Abstract. Recent work has shown that an amorphous drug-polymer salt (ADPS) can be highly stable against crystallization under hot and humid conditions (e.g., 40°C/75% RH) and provide fast release and that these advantages depend on the degree of salt formation. Here we investigate the salt formation between the basic drug lumefantrine (LMF) and several acidic polymers: poly(acrylic acid) (PAA), hypromellose phthalate (HPMCP), hypromellose acetate succinate (HPMCAS), cellulose acetate phthalate (CAP), Eudragit L100, and Eudragit L100-55. Salt formation was performed by "slurry synthesis" where dry components were mixed at room temperature in the presence of a small quantity of an organic solvent, which was subsequently removed. This method achieved more complete salt formation than the conventional methods of hot-melt extrusion and rotary evaporation. The acidic group density of a polymer was determined by non-aqueous titration in the same solvent used for slurry synthesis; the degree of LMF protonation was determined by X-ray photoelectron spectroscopy (XPS). The polymers studied show very different abilities to protonate LMF when compared at a common drug loading, following the order PAA > (HPMCAS ~ CAP ~ L100 ~ L100-55) > HPMCAS, but the difference largely disappears when the degree of protonation is plotted against the concentration of the available acidic groups for reaction. This indicates that the extent of salt formation is mainly controlled by the acidic group density and insensitive to the polymer architecture. Our results are relevant for selecting the optimal polymer to control the degree of ionization in amorphous solid dispersions.

## Introduction

The use of an amorphous solid dispersion (ASD) to deliver poorly soluble drugs<sup>1,2,3</sup> takes advantage of the higher solubility of an amorphous solid relative to its crystals.<sup>4,5,6,7</sup> For an ASD, the stability against crystallization is essential since crystallization negates its advantages.<sup>8,9</sup> In this context, salt formation between a drug and a polymer can effectively inhibit crystallization under hot and humid conditions.<sup>10,11,12,13,14,15</sup> For clofazimine<sup>10</sup> and lumefantrine,<sup>11</sup> the amorphous salts with poly(acrylic acid) also improve release.

The amorphous formulations of the basic drug lumefantrine (LMF) and the acidic polymer poly(acrylic acid) (PAA) have been prepared using several methods <sup>16,17</sup> and the results indicate a strong dependence of salt formation on the methods used and a direct impact on drug stability and release. Using hot-melt extrusion (HME) and rotary evaporation (RE), Song et al. prepared amorphous formulations in which the protonated fractions of LMF molecules were 5% and 15%, respectively, at 40 wt% drug loading.<sup>16</sup> In comparison, a simple slurry-conversion method<sup>10,11</sup> reached 85% protonation at the same drug loading.<sup>17</sup> It was found that the more complete protonation of LMF led to higher stability against crystallization and more complete release into a simulated gastric fluid.<sup>17</sup> These results indicate the critical role of process conditions in preparing ASDs to control their molecular-level structure and performance.

In this work, we build on the previous results to investigate the salt formation between LMF and a series of acidic polymers. Our two questions are: (1) How does the degree of salt formation depend on the polymer structure and properties? and (2) Does the simple slurry method achieve more complete salt formation than the alternative methods for the wide range of polymers? LMF is our model basic drug because of its importance as a WHO Essential Medicine for the first-line treatment of malaria. The low solubility of LMF (BCS Class IV) makes it a candidate for the approach of amorphous formulations to enhance bioavailability. 18 Since malaria is more prevalent in tropical and subtropical countries, product stability under hot and humid conditions is required. making drug-polymer salts a potentially useful formulation strategy. The polymers chosen for this study include: PAA, Eudragit L100, Eudragit L100-55, hypromellose phthalate (HPMCP), cellulose acetate phthalate (CAP), and hypromellose acetate succinate (HPMCAS); see Scheme 1 for their structures. Among these, PAA, L100, and L100-55 feature a simple carbon backbone to which the acidic COOH groups are attached, and the other polymers have a more complex carbohydrate backbone and the COOH group is attached to a sidechain (phthalyl group for HPMCP and CAP, succinyl group for HPMCAS). The diversity of these polymers helps evaluate the role of polymer architecture and acidic group density on salt formation with LMF. We find that the acidic group density of a polymer has a controlling effect on the degree of salt formation at a given drug loading, while the polymer architecture plays a minor role. Furthermore, the simple slurry method achieves significantly more complete salt formation for all the polymers tested than the alternative methods of HME, RE, and spray drying (SD). These results are relevant for selecting polymers for preparing ASDs and predicting the degree of salt formation and formulation performance.

# Acrylic/methacrylic polymers (COOH attached to backbone) LIDO CI PAA LIDO CH3 CH3 HO CH3 R R R H, CH3 or (CH2 O) CH2 R R HO COOH on phthalyl group COOH on succinyl group

**Scheme 1**. Structures of lumefantrine (LMF) and the acidic polymers used for salt formation. The polymers fall into two groups: (1) the acrylic/methacrylic group (PAA, Eudragit L100 and L100-55), where COOH is attached to the carbon backbone, and (2) the cellulosic group, for which COOH is on the sidechain phthalyl group (HPMCP and CAP) or succinyl group (HPMCAS). Eudragit L100 and L100-55 are random copolymers where the x:y ratio is approximately 1.

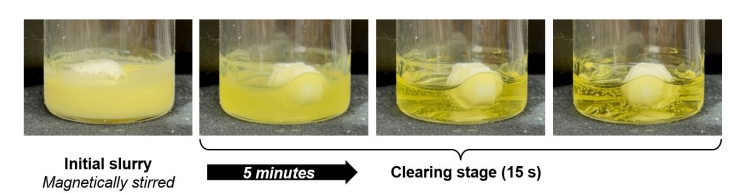
Cellulosic polymers

### **Materials & Methods**

**Materials.** Poly(acrylic acid) (PAA, Carbomer, MW = 450,000 g/mol), cellulose acetate phthalate (CAP, MW = 2,500 g/mol), anhydrous potassium hydroxide (KOH), and phenol red were purchased from Sigma-Aldrich (St. Louis, MO). Eudragit L100 (MW = 125,000 g/mol) and L100-55 (MW = 320,000 g/mol) were purchased from Evonik Industries (Essen, Germany). Hypromellose phthalate (HPMCP-55, MW = 45,600 g/mol) and hypromellose acetate succinate (HPMCAS-LF, HPMCAS-MF, HPMCAS-HF; MW = 17,000 – 20,000 g/mol) were purchased from Shin-Etsu Chemical Company Ltd. (Tokyo, Japan). Lumefantrine was purchased from VWR International (Radnor, PA), dichloromethane (ChromAR grade) from Thermo Fisher Scientific (Fair Lawn, NJ), and ethanol from Decon Laboratories (King of Prussia, PA). All materials were used as received.

**Slurry Synthesis.** The slurry synthesis of amorphous LMF-polymer salts was adapted from the method of Yao et al.<sup>11</sup> and conducted at a reduced temperature of 25 °C (from the original 75 °C). The powders of LMF and a polymer were mixed at a target drug loading (typically 25, 50, 75 wt% and other values as needed) and a mixed solvent of dichloromethane (DCM) and ethanol (1:1 v/v) was added at a solid/liquid ratio of 1:4 (w/w). To prevent gelling of the powder, DCM was

added first followed by ethanol. Each formulation batch contained 400 mg in solid mass. The mixture was stirred magnetically at 25 °C for up to 20 min. During stirring, the initial free-flowing slurry became clear, indicating complete dissolution and amorphization (Scheme 2). The viscous clear solution was dried under vacuum at room temperature for 1 day, resulting in a glassy, brittle foam. The foam was ground in an agate mortar with a pestle to a fine powder for further analysis.



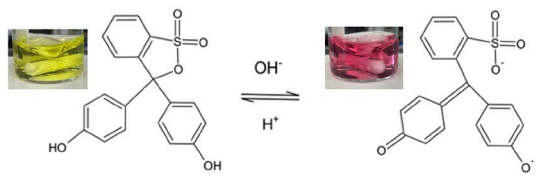
**Scheme 2**. Typical progression of the reaction between LMF and PAA. The left image shows the initial slurry being magnetically stirred. For approximately 5 min, the slurry maintains the cloudy appearance and then abruptly clears. The three images on the right show the abrupt clearing in roughly 15 s. For this preparation, the drug loading was 50 wt%. Similar progression was observed at other drug loading and with other polymers.

**Powder X-ray Diffraction.** X-ray diffraction was performed with a Bruker D8 Advance X-ray diffractometer with a Cu K $\alpha$  source operating at a tube load of 40 kV and 40 mA. A powder sample of approximately 10 mg was spread and flattened on a Si (510) zero-background holder and scanned between 3° and 40° (20) at a step size of 0.02° and a scan rate of 1 s/step. All ASDs were confirmed to be amorphous by the absence of crystalline peaks (Fig. S1).

X-Ray Photoelectron Spectroscopy (XPS). The details of XPS measurement and data analysis have been described previously. For a LMF formulation, approximately 3 mg of a powder was pressed onto a carbon tape fixed to the XPS sample holder. For pure LMF, approximately 1 mg of powder was melted on a glass coverslip and quenched to room temperature by contact with an Al block. The samples were stored in a sealed plastic tube filled with Drierite before XPS analysis. The high-resolution spectrum of the N atom was used to measure the protonated fraction of LMF. For each sample, the spectrum was recorded in duplicate in two separate regions. Curve fitting was performed using the program Origin following smart baseline subtraction.

**Non-aqueous titration.** Colorimetric titration was used to measure the COOH density of each polymer.<sup>21</sup> To be relevant for understanding the drug-polymer reaction, titrations were performed in the same organic solvent used for slurry synthesis. Our method is similar to the USP

analysis for phthalyl content in HPMCP. 12.5 mg of each polymer was dissolved in 25 mL of a 1:1 mixture of DCM and ethanol. To this solution approximately 1 mg of the colorimetric indicator phenol red (Scheme 3) was added and non-aqueous titration was performed with a 0.05 M KOH solution in ethanol as the titrant and the endpoint identified by the color change from yellow to orange.<sup>21,22</sup> Each titration was performed in duplicate.



**Scheme 3**. Phenol red as indicator for non-aqueous acid-base titration. The acidic form of the indicator (left) is yellow and the basic form (right) pink.

### **Results and Discussion**

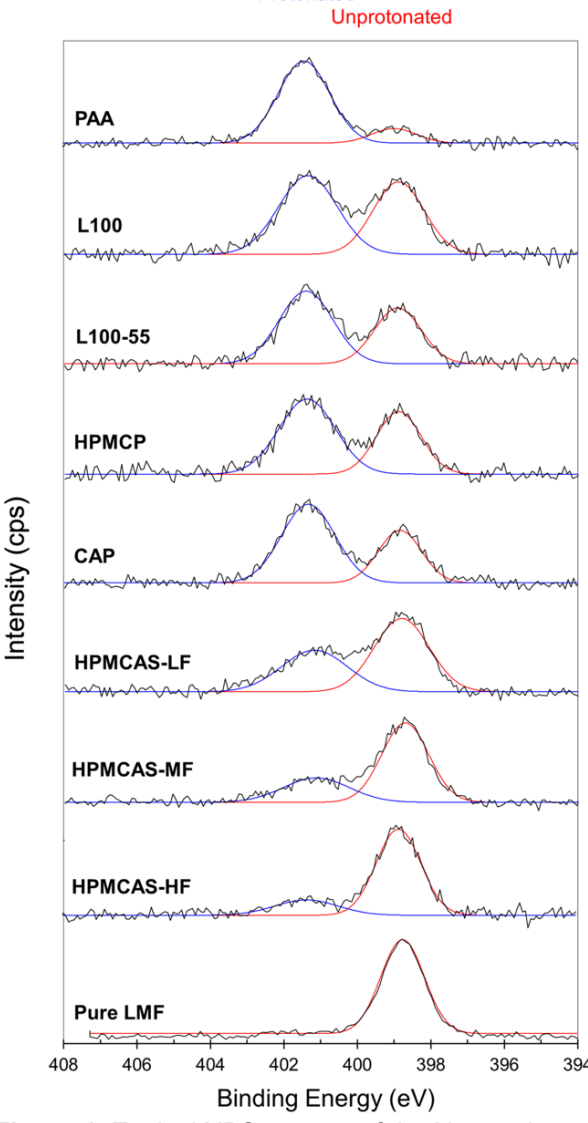
Figure 1 shows the typical XPS spectra of the N atom in LMF in formulations with different acidic

polymers (Scheme 1). For this comparison, the drug loading was 50 wt%. These spectra allowed determination of the extent of salt formation between LMF and the polymer. The pure drug shows a single peak at a binding energy (BE) of 399 eV, corresponding to the unprotonated N atom.<sup>23</sup> Upon reaction with an acidic polymer, a second peak emerges at a higher BE (401.5 eV), corresponding to the protonated N atom. At the fixed DL of 50 wt%, PAA is the most effective in protonating LMF, followed by L100, L100-55, HPMCP, and CAP (no strong differentiation between the latter 4 polymers), and by HPMCAS (three grades). Among the three grades of HPMCAS, the ability to protonate LMF follows the order LF (highest) > MF > HF (lowest).

The degree of protonation (extent of acid-base reaction) is given by:

% N protonated = 
$$\frac{A_P}{A_P + A_N} \times 100$$
 (1)

where  $A_P$  and  $A_N$  are the areas of the protonated and unprotonated (neutral) nitrogen peaks, respectively. We obtain the peak areas by fitting each spectrum as a sum of two Gaussian functions (red and blue curves in Figure 1). Although XPS is a surface-analytical tool, the recorded spectra yield information on salt formation in the bulk since the material had ground to expose internal surfaces and the surface enrichment effect was too slow to occur on the timescale of our measurement.<sup>20</sup>



**Protonated** 

**Figure 1**. Typical XPS spectra of the N atom in LMF formulated with different acidic polymers. For this comparison, drug loading was fixed at 50 wt%. The 399 eV peak corresponds to unprotonated N and the 401.5 eV peak to protonated N. The areas of these peaks areas were used to calculate the degree of protonation of LMF (eq. 1).

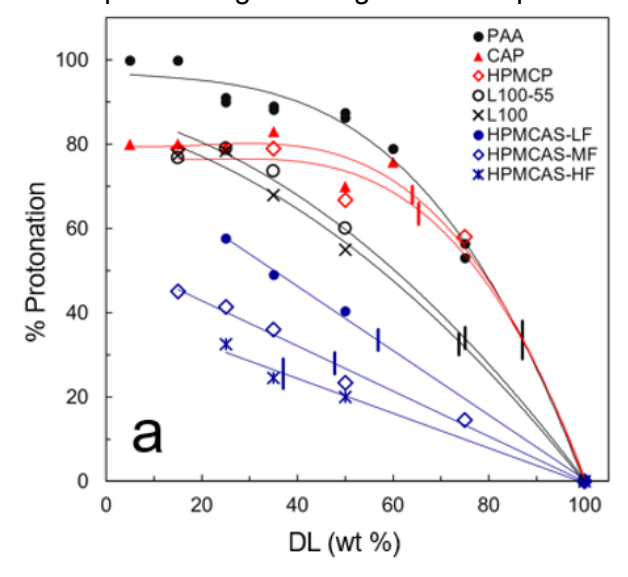
Figure 2a shows the protonated fraction of LMF as a function of DL in the formulations with the different polymers. For each polymer, the % protonation decreases as DL increases. <sup>17</sup> This is because at higher DL, more LMF molecules compete for each reaction site on the polymer chain at lower probability of success. We observe a large difference between the polymers in their ability to protonate LMF. For example, at 50 wt% DL, the degree of protonation is 20% for the reaction with HPMCAS-HF and 87% with PAA. At any DL, PAA is either the most effective in protonating the drug or ties with CAP. The two polymers with PAA-like structures, L100 and L100-55 (see Scheme 1), are significantly less effective than PAA in protonating the drug when compared at

the same DL. Of the polymers tested, the HPMCAS group (three grades) is the least effective in protonating the drug at a given DL, and within this group, the ranking is LF > MF > HF. For the cellulosic polymers, those with COOH on a phthalyl group (HPMCP and CAP) are more able to protonate than those with COOH on a succinyl group (HPMCAS). In Figure 2a, the short vertical line on each curve indicates the DL at which the drug and the polymer's COOH group have equal molar concentrations. This quantity,  $w_0$ , is calculated from the acidic group density of the polymer as discussed below.

In Figure 2b, the % protonation values in Figure 2a are replotted as a function of [COOH]<sub>0</sub>, the COOH concentration in each formulation given by:

$$[COOH]_0 = (1 - DL) [COOH]_p$$
 (2)

where DL is the wt% of LMF (drug loading) and [COOH]<sub>p</sub> is the COOH density of the polymer determined by non-aqueous titration (see below). In this format, the scattered data points in Figure 2a largely coalesce to a single trend, indicating the polymer's acidic group density plays a major role in the degree of salt formation while its architecture a minor role. Below we first discuss the titration results and then return to Figure 2 for further discussion.



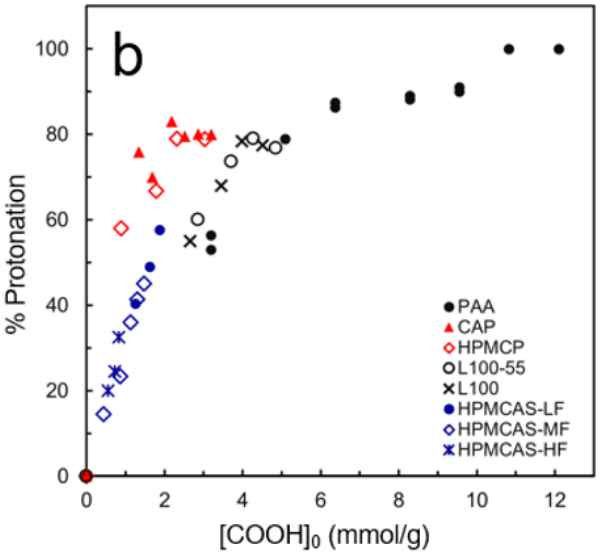


**Figure 2**. (a) Protonated fraction of LMF vs. DL in different polymer formulations. The curves are guide to the eye. The vertical line on each curve indicates the DL,  $w_0$ , at which LMF and the polymer's COOH have the same molar concentration; see Table 1 for the values of  $w_0$ . (b) Protonated fraction of LMF vs. the COOH concentration available for reaction (eq. 2)

Table 1 shows the COOH densities of the polymers determined by non-aqueous titration. From the titrant volume at the endpoint (Column 2), the COOH density was calculated (Column 3). The titrations were performed in the same organic solvent as used for slurry synthesis (1:1 DCMethanol) rather than the standard medium of water to ensure accurate measurement of accessible acidic groups in the reaction medium. This is important as the strength of an acid or base depends on its solvent environment.<sup>21</sup> For a polymer, the solvent has a strong influence on its conformation and accessible reaction sites. 24,25 For the polymers tested, PAA has the highest COOH density, and the two structurally similar polymers, L100 and L100-55, have lower densities, as expected. For the cellulosic polymers, HPMCP and CAP have higher COOH densities than HMPCAS. The measured COOH density for PAA, 12.7 (0.09) mmol/g, is reasonably close to the theoretical value of 13.9 mmol/g and the small difference could result from deviations from the ideal polymer structure (e.g., small degree of crosslinking). Of the three HPMCAS grades, the COOH densities follow the order LF > MF > HF and are in quantitative agreement with their succinyl contents.<sup>26</sup> Since the COOH groups in HPMCAS reside on the succinvl sidechain, its density should be proportional to the succinvl content. This is indeed observed (Figure 3) and validates our titration method to determine the acidic group density in a polymer.

**Table 1**. COOH densities of polymers determined by non-aqueous titration in the same solvent used for slurry synthesis.

Polymer	V KOH (µL)	[COOH] <sub>p</sub> (mmol/g)	Succinyl Content (%)	w <sub>0</sub> (wt %)
PAA	3183 (24)	12.7 (0.09)	-	87
Eudragit L100-55	1425 (20)	5.70 (0.08)	-	75
Eudragit L100	1328 (8)	5.31 (0.03)	-	74
НРМСР	890 (29)	3.56 (0.04)	-	65
CAP	840 (11)	3.36 (0.04)	-	64
HPMCAS-LF	622 (9)	2.49 (0.03)	14 – 18	57
HPMCAS-MF	433 (13)	1.73 (0.05)	10 – 14	48
HPMCAS-HF	277 (14)	1.11 (0.06)	4 – 8	37

Knowing the acidic group density of each polymer, [COOH]<sub>p</sub>, it is possible to calculate the DL at which the drug has the same molar concentration as the COOH group in the polymer:

$$w_0 = 100 M_0 [COOH]_p / (1 + M_0 [COOH]_p)$$
 (3)

where  $M_0$  is the molar mass of the drug LMF (528.9 g/mol). The calculated values are given in Table 1. These values provide further validation of the titration method. For example, for PAA,  $w_0$  can be calculated from the molar masses of LMF and the AA monomer (72.1 g/mol). The result, 88 wt %, agrees with the value from titration (87 wt %). The difference could be a result of the experimental error and/or deviation of the actual polymer structure from the ideal structure.

In Figure 2a, we indicate the  $w_0$  value for each polymer formulation with a short vertical line. At DL <  $w_0$ , there are enough COOH groups to neutralize all the drug molecules; at DL >  $w_0$ , the opposite is true. The data do not indicate any sharp transition as DL traverses  $w_0$  and even when the COOH groups are in excess, it is generally impossible to fully protonate the drug.

In Figure 2b, we plot the same data in Figure 2a against [COOH]<sub>0</sub>, the COOH concentration available for reaction calculated from the titration results using eq. 2. In this format, the scatter seen in Figure 2a mostly disappears and the data points cluster around a single trend. This indicates that the degree to which LMF is protonated is mainly controlled by the COOH density of the polymer and is less sensitive to its architecture. This conclusion is by no means obvious. For example, if we compare the structures of PAA, L100 and L100-55 (Scheme 1), we might speculate that the larger spacing between COOH groups in L100 and L100-55 allow these polymers to react more efficiently with the drug, leading to higher % protonation at the same [COOH]<sub>0</sub>. But we observe no the three polymers reach approximately the same % protonation and the same groups in the same % protonation at the same proximately the same % protonation at the same same proximately the same % protonation at the same same proximately the same % protonation at the same same proximately the same % protonation at the same same proximately the same % protonation at the same same proximately the same % protonation at the same same proximately the same % protonation at the same same proximately the same same proximately the same % protonation at the same same proximately the same same same proximately the same proximately the same same proxima

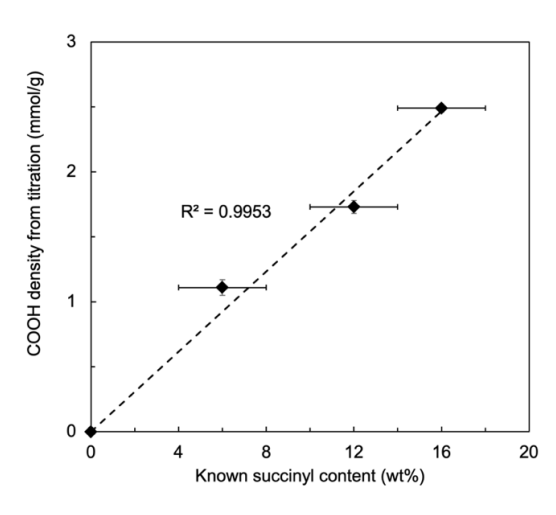


**Figure 3**. [COOH]<sub>p</sub> of each HPMCAS grade (LF, MF, or HF) plotted against its succinyl content (range indicated as horizontal bar). The two quantities are proportional to each other, as expected, indicating the titration method correctly determines the acidic group density.

protonation at the same [COOH]<sub>0</sub>. But we observe no such effect in Figure 2b (black symbols): the three polymers reach approximately the same % protonation at a common [COOH]<sub>0</sub> (e.g., 5 mmol/g). Thus, despite their different architectures, each COOH in these polymers has approximately the same reactivity toward LMF.

The trend formed by PAA, L100, and L100-55 appears to smoothly join the data points for HPMCAS (3 grades). This further indicates that the polymer's architecture plays a relatively minor role in its reaction with LMF. In PAA, L100, and L100-55, the COOH group is directly attached to the polymer's carbon chain, whereas in HPMCAS, the COOH group is attached to a succinyl side chain of a complex cellulose backbone. Despite this difference, each COOH group has a similar reactivity toward LMF. Interestingly, relative to this trend, HPMCP and CAP appear to be more potent protonators. In these polymers, COOH is attached to a phthalyl sidechain of the cellulose backbone. Overall, the main conclusion from Figure 2b is that the polymer's COOH density has a stronger effect on the salt formation with LMF than its architecture. It would be of interest to model these systems by molecular simulations to learn how the molecules organize themselves to achieve this.

To complete the characterization of our systems, in Figures 4, we show the fraction of the COOH groups that are deprotonated in each formulation as a function of DL. This quantity is calculated from:

% deprotonation = 
$$[LMF]_0$$
 (% protonation) /  $[COOH]_0$  (4)

where [LMF]<sub>0</sub> is the initial concentration of the drug, % protonation is the protonated fraction of LMF after reaction, and [COOH]<sub>0</sub> is the initial concentration of COOH (eq. 2). For each system, increasing the DL increases the % deprotonation of the polymer. These results complement those in Figure 2a, which indicate a decrease of the % protonation of the drug with increasing DL. Note in Figure 4 that at the same DL, the acrylic/methacrylic polymers (PAA, L100, and L00-55, in black

symbols) show lower % deprotonation than the cellulosic polymers (red and blue symbols). Within the cellulosic polymers, those with the COOH on a phthalyl group (CAP and HPMCP) deprotonated to a greater extent at DL > 50% than those with the COOH on a succinyl group (HPMCAS in three grades). At DL = 75 wt %, HPMCP is almost fully deprotonated, while HPMCAS-MF is 50% deprotonated. This difference is consistent with the view that HPMCP and CAP are slightly stronger acids than HPMCAS and with their greater protonating power seen in Figure 2b near  $[COOH]_0 = 2 \text{ mmol/g}$ .

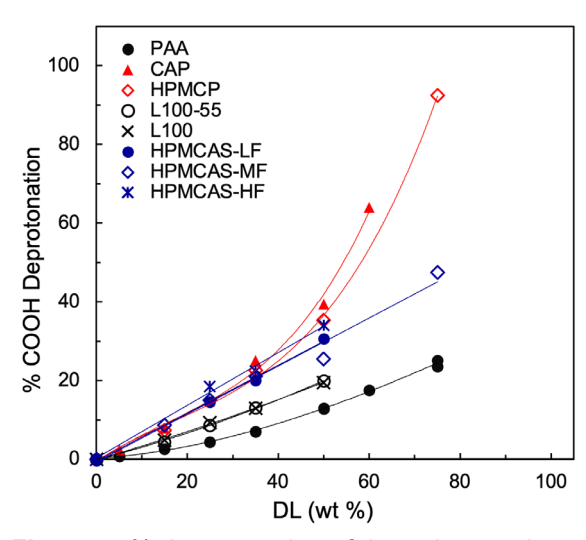


**Figure 4**. % deprotonation of the polymer when formulated with LMF as a function of DL.

### Comparison of ASD Manufacturing Methods.

Several methods have been used to prepare amorphous LMF-polymer formulations, including HME, <sup>16</sup> SD, <sup>16</sup> RE, <sup>16,27,13</sup> and slurry conversion (SC). <sup>11,17</sup> Table 2 summarizes the attributes of these methods and Figure 5 compares the degrees of salt formation reached by them. Among these methods, HME does not require any solvent, while the others do. For the solvent-based methods, SC uses less solvent (4:1 solvent/solid ratio) than SD and RE (50:1). As for the reaction temperature, HME employs a higher temperature (130 °C) than the solvent-based methods (room temperature, though reaction can also occur during spray drying at elevated temperature). In the drying stage, SD requires a higher temperature than RE and SC and between the latter two methods, drying is significantly faster for SC since less solvent must be removed.

**Table 2**. Comparison of the methods used to prepare amorphous LMF-polymer formulations.

	Hot melt extrusion (HME) <sup>16</sup>	Spray drying (SD) <sup>16</sup>	Rotary evaporation (RE) 27,16	Slurry conversion (SC) <sup>11,17</sup>
Solvent	None	DCM-methanol (1:1)	DCM-methanol (1:1 or 8:2), DCM- ethanol (1:1)	DCM-ethanol (1:1)
Solvent/solid ratio	NA	50:1	50:1	4:1
Reaction temperature	130 °C	RT (higher T during drying)	RT (45 °C during drying)	RT default, 75 °C also used
Drying	NA	75 °C inlet, 45 °C outlet	45 °C under vacuum	RT under vacuum

Note. RT: room temperature

Figure 5 compares the % protonation of LMF in polymer formulations prepared by the different methods. The PAA and L100-55 systems allow comparison of SC (solid circles) with HME (crosses) and we find that HME achieves less complete salt formation than SC, by a factor of 3 – 18. Similarly, we can use the L100-55, HPMCP, and HPMCAS-MF formulations to evaluate the relative performance of SC and SD (open circles). For the L100-55 and HPMCP systems, SD

reaches similar degrees of salt formation as SC; for the HPMCAS-MF system, SD significantly underperforms SC, yielding no salt formation. Finally, every system in Figure 5 except for L100-55 allows a comparison of SC with RE (open triangles) and in every case, RE significantly underperforms SC, by up to a factor of 2. Overall, these results indicate that SC has the best performance for completing the salt formation between LMF and an acidic polymer. Apart from this metric, SC has the advantage of lower solvent consumption than SD and RE and lower operating temperature than SD, making it a low-cost and green alternative to the current manufacturing platforms.

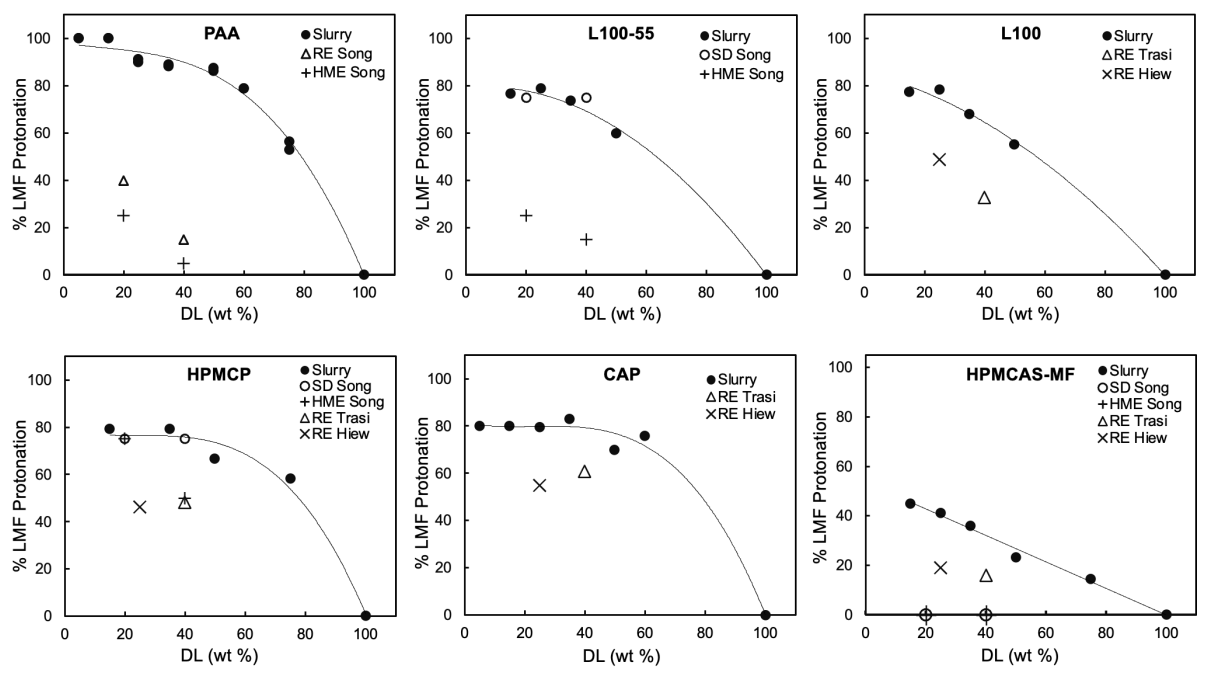


**Figure 5**. Comparison of % protonation of LMF in formulations with different polymers prepared with different methods. "Slurry" refers to the slurry conversion (SC) method used in this work. HME: hot melt extrusion. SD: spray drying. RE: rotary evaporation.

At present, it is not well understood why the different manufacturing methods reach different degrees of salt formation between LMF and an acidic polymer. The underperformance of HME relative to the solution-based methods suggests the need for a solvent in completing the reaction. A solvent could be a mass-transfer aide that helps complete salt formation. Given that a liquid surfactant is commonly present in HME-prepared ASDs, it is of interest to learn whether the addition of a surfactant could promote salt formation. The outperformance of SC over other solvent-based methods is more puzzling since they all begin with a homogeneous solution and involve the drying of that solution. In SC, the initial solution is more concentrated than in SD and RE. A more concentrated solution could facilitate the formation of ion pairs, the principal species for ions in an organic solvent, 21 since ion pairs tend to dissociate in a dilute solution and revert to neutral molecules. This hypothesis can be tested with NMR measurements. It is also possible that depending on the drying conditions, the system evolves on different paths before kinetic arrest (glass transition), leading to different products. The very different molecular structures of the formulations prepared by the different methods account for the large difference in their stability and performance. 17 Future work is needed to help define the optimal manufacturing methods and conditions for high performing ASDs.

### **Conclusions**

This study investigated the salt formation between the basic drug lumefantrine (LMF) and a series of acidic polymers based on acrylic/methacrylic and cellulosic backbones (Scheme 1). The polymers show very different abilities to protonate LMF when compared at the same drug loading (DL) (Figure 2a), but the difference largely disappears when the results are plotted against the COOH concentration available for reaction (Figure 2b). This indicates that for the polymers tested, the abilities to protonate LMF depend mainly on their acidic group densities and are less sensitive to their architectures. For this analysis, the acidic group densities were determined by non-aqueous titration in the same medium used for slurry synthesis to accurately probe the accessible reaction sites. Had the aqueous titration results<sup>13</sup> been used in this analysis, data collapse would be less complete. Our finding that a polymer's COOH density outweighs its architecture in predicting salt formation with a basic drug is relevant for polymer selection in developing amorphous formulations. This conclusion is by no means obvious; it is even counterintuitive for PAA, L100, and L100-55 taken as a group, since the wider spacing of COOH groups in L100 and L100-55 might suggest higher reactivity with the drug, contrary to the experimental results (Figure 2b). Future work is warranted to understand why the crowding effect is seemingly unimportant.

The second part of this work has compared the slurry synthesis used here with three other methods for manufacturing amorphous drug-polymer formulations. For LMF reacting with the 6 polymers, slurry conversion either achieves the most complete salt formation (4 of 6 polymers) or ties with spray drying for the first place (2 of 6). Compared to spray drying, slurry conversion has lower cost, lower solvent consumption, and lower drying temperature. This encourages further development of the method for broader applications as a platform to manufacture amorphous solid dispersions. A remarkable result from this comparison is that for a given amorphous formulation (with a specific polymer at a specific DL), the internal structures can be vastly different, depending on the methods of preparation (Figure 5). The common method of hot-melt extrusion consistently yielded the lowest degree of salt formation. Spray drying showed comparable performance as slurry conversion for two polymers, but yielded no reaction for a third. Rotary evaporation, in principle a similar method to slurry conversion, consistently yielded less complete salt formation than slurry conversion. The amorphousness of a multi-component formulation might suggest intimate mixing and reaction of its components, but a detailed analysis like the degree of protonation can reveal large structural differences, with direct impact on stability and dissolution kinetics.<sup>17</sup> To obtain a consistent product with a reproducible molecular-level structure, the manufacturing process must be carefully chosen and controlled. This task is not unlike the control of polymorphism for crystalline materials and requires analytical tools that go beyond the amorphous halo of X-ray diffraction.

# Acknowledgements

This work was supported by the Bill and Melinda Gates Foundation (OPP1160408) and we acknowledge the helpful discussions with Niya Bowers, David Monteith, and Paco Alvarez. Under the grant conditions of the Foundation, a Creative Commons Attribution 4.0 Generic License has already been assigned to the Author Accepted Manuscript version that might arise from this submission. The data that support the findings of this study are openly available in Mendeley Data at doi:10.17632/ s23j9y3mc8.1. The authors acknowledge the use of the characterization facility of the NSF-supported University of Wisconsin Materials Research Science and Engineering Center (DMR- 2309000).

### References

\_

- <sup>1</sup> Mishra, D. K.; Dhote, V.; Bhargava, A.; Jain, D. K.; Mishra, P. K. Amorphous Solid Dispersion Technique for Improved Drug Delivery: Basics to Clinical Applications. *Drug Delivery and Translational Research* **2015**, *5* (6), 552–565.
- <sup>2</sup> Baghel, S.; Cathcart, H.; O'Reilly, N. J. Polymeric Amorphous Solid Dispersions: A Review of Amorphization, Crystallization, Stabilization, Solid-State Characterization, and Aqueous Solubilization of Biopharmaceutical Classification System Class II Drugs. *Journal of Pharmaceutical Sciences* **2016**, *105* (9), 2527–2544.
- <sup>3</sup> He, Y.; Ho, C. Amorphous Solid Dispersions: Utilization and Challenges in Drug Discovery and Development. *Journal of Pharmaceutical Sciences* **2015**, *104* (10), 3237–3258.
- <sup>4</sup> Murdande, S. B.; Pikal, M. J.; Shanker, R. M.; Bogner, R. H. Solubility Advantage of Amorphous Pharmaceuticals: I. A Thermodynamic Analysis. *Journal of Pharmaceutical Sciences* **2010**, *99* (3), 1254–1264
- <sup>5</sup> Babu, N. J.; Nangia, A. Solubility Advantage of Amorphous Drugs and Pharmaceutical Cocrystals. *Crystal Growth & Design* **2011**, *11* (7), 2662–2679.
- <sup>6</sup> Chawla, G.; Bansal, A. K. A Comparative Assessment of Solubility Advantage from Glassy and Crystalline Forms of a Water-Insoluble Drug. *European Journal of Pharmaceutical Sciences* **2007**, *32* (1), 45–57.
- <sup>7</sup> Hancock, B. C.; Parks, M. What Is the True Solubility Advantage for Amorphous Pharmaceuticals? *Pharmaceutical Research* **2000**, *17* (4), 397–404.
- <sup>8</sup> Newman, A.; Knipp, G.; Zografi, G. Assessing the Performance of Amorphous Solid Dispersions. *Journal of Pharmaceutical Sciences* **2012**, *101* (4), 1355–1377.
- <sup>9</sup> Shah, N.; Iyer, R. M.; Mair, H.-J.; Choi, D.; Tian, H.; Diodone, R.; Fahnrich, K.; Pabst-Ravot, A.; Tang, K.; Scheubel, E.; Grippo, J. F.; Moreira, S. A.; Go, Z.; Mouskountakis, J.; Louie, T.; Ibrahim, P. N.; Sandhu, H.; Rubia, L.; Chokshi, H.; Singhal, D. Improved Human Bioavailability of Vemurafenib, a Practically Insoluble Drug, Using an Amorphous Polymer-Stabilized Solid Dispersion Prepared by a Solvent-Controlled Coprecipitation Process. *Journal of Pharmaceutical Sciences* **2013**, *102* (3), 967–981.
- <sup>10</sup> Gui, Y.; McCann, E. C.; Yao, X.; Li, Y.; Jones, K. J.; Yu, L. Amorphous Drug–Polymer Salt with High Stability under Tropical Conditions and Fast Dissolution: The Case of Clofazimine and Poly(Acrylic Acid). *Molecular Pharmaceutics* **2021**, *18* (3), 1364–1372.
- <sup>11</sup> Yao, X.; Kim, S.; Gui, Y.; Chen, Z.; Yu, J.; Jones, K. J.; Yu, L. Amorphous Drug–Polymer Salt with High Stability under Tropical Conditions and Fast Dissolution: The Challenging Case of Lumefantrine-PAA. *Journal of Pharmaceutical Sciences* **2021**, *110* (11), 3670–3677.
- <sup>12</sup> Yao, X.; Neusaenger, A. L.; Yu, L. Amorphous Drug-Polymer Salts. *Pharmaceutics* **2021**, *13* (8), 1271.
- <sup>13</sup> Hiew, T. N.; Zemlyanov, D. Y.; Taylor, L. S. Balancing Solid-State Stability and Dissolution Performance of Lumefantrine Amorphous Solid Dispersions: The Role of Polymer Choice and Drug–Polymer Interactions. *Molecular Pharmaceutics* **2021**, *19* (2), 392-413.
- <sup>14</sup> Kelsall, K. N., Foroughi, L. M., Frank, D. S., Schenck, L., LaBuda, A., & Matzger, A. J. (2023). Structural Modifications of Polyethylenimine to Control Drug Loading and Release Characteristics of Amorphous Solid Dispersions. *Molecular Pharmaceutics*, 20 (3), 1779–1787.

<sup>15</sup> Kelsall, K. N., Schubiner, R. O., Schenck, L., Frank, D. S., & Matzger, A. J. (2024). Enhancing the Acidity of Polymers for Improved Stabilization of Amorphous Solid Dispersions: Protonation of Weakly Basic Compounds. *ACS Applied Polymer Materials*, (6) 3, 1592–1598.

- <sup>16</sup> Song, Y.; Zemlyanov, D.; Chen, X.; Su, Z.; Nie, H.; Lubach, J. W.; Smith, D.; Byrn, S.; Pinal, R. Acid-Base Interactions in Amorphous Solid Dispersions of Lumefantrine Prepared by Spray-Drying and Hot-Melt Extrusion Using X-Ray Photoelectron Spectroscopy. *International Journal of Pharmaceutics* **2016**, *514* (2), 456–464.
- <sup>17</sup> Amy Lan Neusaenger; Yao, X.; Yu, J.; Kim, S.; Hui, H.-W.; Huang, L.; Que, C.; Yu, L. Amorphous Drug–Polymer Salts: Maximizing Proton Transfer to Enhance Stability and Release. *Molecular Pharmaceutics* **2023**, *20* (2), 1347–1356.
- <sup>18</sup> Jain, J.P.; Leong, F.J.; Chen, L.; Kalluri, S.; Koradia, V.; Stein, D.S.; Wolf, M.C.; Sunkara, G.; Kota, J. Bioavailability of lumefantrine is significantly enhanced with a novel formulation approach, an outcome from a randomized, open-label pharmacokinetic study in healthy volunteers. *Antimicrob. Agents Chemother.* **2017**. *61*(9).
- <sup>19</sup> Evonik. (**2022**). *Eudragit*®, [Technical Literature] Evonik Industries AG.
- <sup>20</sup> Yu, J.; Li, Y.; Yao, X.; Que, C.; Huang, L.; Hui, H.-W.; Gong, Y.; Qian, F.; Yu, L. Surface Enrichment of Surfactants in Amorphous Drugs: An X-Ray Photoelectron Spectroscopy Study. *Molecular Pharmaceutics* **2022**, *19* (2), 654–660..
- <sup>21</sup> Marion Maclean Davis. *Acid-Base Behavior in Aprotic Organic Solvents*; U.S. Department of Commerce National Bureau of Standards, 1968.
- <sup>22</sup> Shen, X.; Wang, S.; Qian Lü; Guo, Y.; Li, Q. Translating Cancer Exosomes Detection into the Color Change of Phenol Red Based on Target-Responsive DNA Microcapsules. *Analytica Chimica Acta* **2022**, *1192*, 339357–339357.
- <sup>23</sup> He, H., Hu, Y., Chen, S. *et al.* Preparation and Properties of a Hyperbranch-Structured Polyamine adsorbent for Carbon Dioxide Capture. *Sci Rep* **2017**, *7*, 3913.
- <sup>24</sup> Amirdehi, M. A.; Pousti, M.; Asayesh, F.; Gharib, F.; Greener, J. Solvent Effects on Acid–Base Equilibria of Propranolol and Atenolol in Aqueous Solutions of Methanol: UV-Spectrophotometric Titration and Theory. *Journal of Solution Chemistry* 2017, 46, 720–733.
- <sup>25</sup> Sappidi, P., & Natarajan, U. (2016). Polyelectrolyte conformational transition in aqueous solvent mixture influenced by hydrophobic interactions and hydrogen bonding effects: PAA–water–ethanol. *Journal of Molecular Graphics and Modelling*, *64*, 60–74. https://doi.org/10.1016/j.jmgm.2015.12.004
- <sup>26</sup> Ashland. (**2016**). *AquaSolve™ hydroxypropylmethylcellulose acetate succinate: Physical and chemical properties handbook*, [Technical Literature] Ashland Global.
- <sup>27</sup> Trasi, N. S.; Bhujbal, S. V.; Zemlyanov, D. Y.; Zhou, Q. T.; Taylor, L. S. Physical stability and release properties of lumefantrine amorphous solid dispersion granules prepared by a simple solvent evaporation approach. *International Journal of Pharmaceutics: X* **2020**, *2*, 100052.